

Tip-Angle-Reduced T_1 Imaging

T. H. MARECI,*† W. SATTIN,*‡ AND K. N. SCOTT*†‡§

*Departments of *Radiology, †Physics, and ‡Nuclear Engineering Sciences, University of Florida, and §V.A. Medical Center, Gainesville, Florida 32610*

AND

AD BAX

Laboratory of Chemical Physics, National Institutes of Health, Bethesda, Maryland 20205

Received August 19, 1985

A new imaging technique is introduced which provides a series of stimulated echo images progressively weighted with T_1 relaxation with constant T_2 weighting. The series of T_1 -weighted images is acquired during a single imaging sequence in a manner similar to a conventional T_2 -weighted spin-echo imaging sequence. A 90° pulse creates transverse magnetization which is phase encoded and stored along the longitudinal axis by a 90° storage pulse. The image information is acquired by obtaining a series of stimulated echoes, each following a read pulse, which samples residual longitudinal magnetization not recovered to equilibrium. The tip angles of the read pulses are adjusted to given equal tip-angle weighting for each image. This is accomplished by making the tip angle of the first read pulse small and increasing the tip angle of each succeeding pulse, in a recursive manner, so that the last pulse in the series has a tip angle of 90° . This imaging method is dubbed tip-angle-reduced T_1 (TART) imaging. © 1986 Academic Press, Inc.

INTRODUCTION

There are many methods of imaging the structure of an object of interest. One can rely on optical transmission or reflection of light in conventional microscopy, scattering of electrons by an object in electron microscopy, or X-ray transmission in plane or tomographic radiography. All these techniques use the transmission or reflection of incident radiation to create an image. In contrast, the technique of imaging with nuclear magnetic resonance is based on a fundamentally different process. A spatial dependence of the nuclear magnetic resonance frequency is created by imposing linear gradients on the main magnetic field. Hence the information contained in such an image is quite different from that obtained with the techniques mentioned above. The density of spins is represented by equilibrium magnetization and the local magnetic environment of the spins by the characteristic relaxation times.

The spatial resolution of nuclear magnetic resonance imaging is limited by the inherent signal strength, magnet inhomogeneities, and the ability to construct strong, linear field gradients which can respond in an appropriate time scale for an imaging technique. The resolving power of nuclear magnetic resonance imaging is sufficient

to place the method in a microscopic category; however, resolution will probably be limited to the order of tens of microns (*1*). Although the resolution of nuclear magnetic resonance imaging is good, it is not dramatically better than other methods of imaging. The advantage of nuclear magnetic resonance imaging is in the type of information available. Aside from spatially mapping the density of spins, nuclear magnetic resonance imaging can also represent a contrast due to relaxation differences between areas of the region imaged. This has proven extremely useful in medical diagnosis where contrast difference can be used to represent an area of pathological tissue (*2*). It is possible that relaxation differences in an image can be used to reflect local structural changes in materials other than biological tissue.

Currently, relaxation differences between areas of an image are enhanced by use of either the conventional inversion-recovery (*3*) or spin-echo (*4*) technique to weight the image according to the choice of pulse sequence parameters. A sequence of T_2 -weighted images can be acquired in a single imaging experiment by collecting image data after each refocusing pulse during a Carr-Purcell-Meiboom-Gill spin-echo sequence (*5*). Each image is progressively more weighted by T_2 relaxation as the echo time increases. Thus a clear indication of T_2 differences can be mapped out by this series of images. A similar sequence is not available for T_1 weighting. Only a single T_1 weighting can be introduced into an image or T_2 -weighted series of images. This is accomplished by providing an initial condition which is T_1 weighted by either an inversion-recovery sequence or rapidly repeated spin-echo sequence. Thus to map T_1 weighting requires several repeated measurements of the image with a variation of a parameter which produces a T_1 weighting.

It is desirable to have an imaging technique which could produce a series of T_1 -weighted images from one imaging sequence. This would provide a great savings in time and the information obtained would compliment that obtained from the T_2 -weighted spin-echo series of images. In this article, we would like to introduce an imaging technique which produces such a series of T_1 -weighted images in a single imaging sequence. The images are acquired as multiple stimulated echoes (*6*) in a single imaging sequence. The resultant series of images are exponentially weighted as a function of T_1 , each with equal T_2 weighting. The sequence requires a series of rf pulses equal to or less than 90° so the sequence can be easily generalized to multislice, multiecho acquisition without the attendant problems of slice selection with pulses greater than 90° .

DESCRIPTION OF THE TECHNIQUE

Earlier work with stimulated echo imaging (*7*) demonstrated the utility of storing phase encoded magnetization along the longitudinal axis thus providing T_1 weighting for the later observation of stimulated echo images. The imaging sequence can be repeated with a variation of the storage time to introduce T_1 weighting in a similar manner to either inversion-recovery or spin-echo imaging. It is also possible to observe a series of stimulated echo images within one imaging sequence with a series of 90° read pulses. The number of echoes produced after each read pulse increases as the number of pulses increases. Also the echo amplitudes have an increasingly complex dependence on the tip angle of the read pulse and mixed weighting due to T_1 and T_2 relaxation during interpulse intervals. This complex result can be greatly simplified

by using a series of read pulses, each less than or equal to 90° , chosen to provide equal tip-angle weighting for each observed image in the series. The observed stimulated echo for each image is derived from the same storage and read mechanisms. Thus, the weighting due to relaxation is simplified while other echoes are suppressed with pulsed field gradients.

This approach is based on earlier work for the observation of either T_1 relaxation (8) or zero-quantum coherence (9) in a single pulse sequence. In both these cases, the spin system was initially prepared into the desired state and its time evolution observed with a series of read pulses small enough to only slightly perturb the evolving state. In the stimulated echo imaging technique described here, the first 90° pulse creates transverse magnetization which dephases in the inhomogeneous static field and is phase encoded with applied linear field gradients. The second 90° pulse splits the transverse magnetization into two equal parts. One portion remains as transverse magnetization forming an echo following the second 90° pulse. The other portion is stored as longitudinal magnetization which retains phase memory of the time evolution between the first two pulses. This stored longitudinal magnetization will relax to equilibrium with the usual time constant, T_1 . If this stored magnetization is sampled with a read pulse before complete recovery to equilibrium has occurred, a stimulated echo is formed which retains phase encoded information and can be used to form an image. The residual longitudinal magnetization is reduced by the effect of the read pulse. For a series of read pulses, each less than or equal to 90° , the observed stimulated echo after each pulse can be used to form an image which has T_1 weighting dependent on the time interval between the 90° storage pulse and the specific read pulse which produces the echo of interest. A specific pulse sequence to produce a series of T_1 -weighted stimulated echo images is shown in Fig. 1 with the pulse phase cycle given in Table 1. The choice of small tip-angle read pulses leads to a series of T_1 -weighted images so this method has been dubbed, tip-angle reduced T_1 (TART) imaging.

The amount of transverse relaxation is the same for each image in the sequence of Fig. 1. Here it is assumed that the read gradient, g_x , is adjusted such that the echo due to magnet inhomogeneities and applied gradients occur at the same point in time. The storage pulse splits the magnetization into two equal parts; one portion forming the primary echo and the other stored as longitudinal magnetization. The primary echo following the 90° storage pulse will occur at a time, TE, after the slice selective 90° pulse which creates transverse magnetization. Ignoring diffusion and assuming ideal 90° pulses, the primary echo signal amplitude can be written as,

$$S_{PE} = \frac{1}{2}M_0e^{-TE/T_2}, \quad [1]$$

where M_0 is the equilibrium magnetization. The factor of one-half comes from the splitting of the transverse magnetization into two equal parts by the 90° storage pulse.

The residual longitudinal magnetization after a stimulated echo read pulse is reduced by a factor of the cosine of the read pulse tip angle. Hence the magnetization available to the next read pulse is reduced in magnitude. The tip-angle dependence of the signal intensity following the n th stimulated echo read pulse can be written as

$$S_n \sim \sin \alpha_n \left(\prod_{i=1}^{n-1} \cos \alpha_i \right), \quad [2]$$

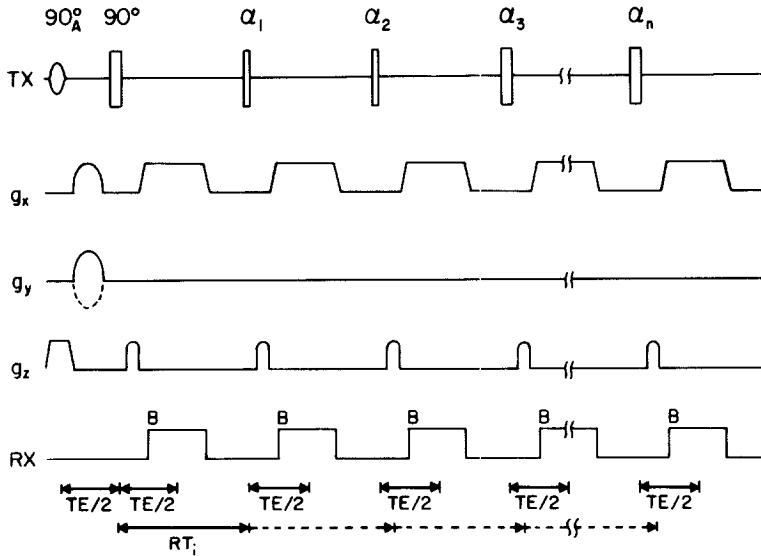


FIG. 1. Tip-angle-reduced T_1 (TART) imaging pulse sequence. This version of the sequence is slice selective perpendicular to the z axis and can be used to create an xy -planar image by two-dimensional Fourier transformation. TE is the time to echo and RT_i , the recovery time between the storage pulse and the i th read pulse.

where the i th read pulse tip angle is denoted as α_i . The relative intensity of signals following each read pulse can be made independent of pulse tip angles by equating the $n - 1$ and n th signal (10), as described by Eq. [2],

$$\sin \alpha_n \left(\prod_{i=1}^{n-1} \cos \alpha_i \right) = \sin \alpha_{n-1} \left(\prod_{i=1}^{n-2} \cos \alpha_i \right). \quad [3]$$

A recursive relationship can be generated for successive tip angles as,

$$\alpha_{n-1} = \arctan(\sin \alpha_n). \quad [4]$$

Since the last pulse in the series should be 90° to maximize the observable signal intensity, one can choose this as a starting point to generate the sequence of read pulse

TABLE I
Four-Step Phase Cycle^a

Number of averages	A	B
1	0°	0°
2	270°	90°
3	180°	180°
4	90°	270°

^a The phase of the selective 90° pulse is denoted A and the phase of the receiver, B.

tip angles. A sequence of four read pulse tip angles satisfying Eq. [4] are shown in Table 2. These are the last four tip angles in any sequence and the series can be extended to any number of read pulses. Note that the observable signal intensity after each read pulse will decrease as the number of read pulses increases. The relative intensity of the observed signal in each image will be independent of the number of read pulses; however, the available signal-to-noise in each image will decrease as the number increases. Thus a practical limit will be reached dependent on the sensitivity of the imaging system.

Since the storage pulse occurs at $TE/2$, the stimulated echo occurs at a time $TE/2$ after the read pulse. Therefore the transverse relaxation weighting of each echo following a read pulse will be equal to that of the primary echo. Since the stored longitudinal magnetization is only affected by T_1 relaxation, the amount of T_1 relaxation for each stimulated echo is only dependent on the recovery time, RT , that has elapsed since the magnetization was initially stored along the longitudinal axis. The stimulated echo amplitude following the n th read pulse has relaxation weighting given by

$$S_n \sim e^{-TE/T_2} e^{-RT_n/T_1}. \quad [5]$$

The effect of relaxation and tip-angle variation can be combined to give the stimulated echo amplitude following the n th read pulse,

$$S_n = \frac{1}{2} M_0 \sin \alpha_n \left(\prod_{i=1}^{n-1} \cos \alpha_i \right) e^{-TE/T_2} e^{-RT_n/T_1}. \quad [6]$$

The reduced tip angles of the read pulses result in a reduction in available signal-to-noise ratio in the final images. This decrease in signal strength can be kept at a tolerable level by limiting the number of read pulses applied to create a T_1 -weighted series of images. The four-pulse example of Table 2, results in a signal reduction for each stimulated echo image to 0.5 that of the primary echo image due to the reduced tip angle of the read pulses. Ignoring relaxation effects, this is an overall reduction in signal strength to 0.25 of the equivalent Carr–Purcell T_2 -weighting series of images. The loss of signal strength does not increase dramatically as the number of read pulses increase because of the functional form of the tip-angle dependence. For example, the

TABLE 2

Final Four Tip Angles in a Series
of n Read Pulses

Number of read pulse	Tip angle ^a
$n - 3$	30°
$n - 2$	35.3°
$n - 1$	45°
n	90°

^a Tip angles were calculated from Eq. [4] assuming the last read pulse tip angle equals 90° .

T_1 -weighted series can be extended to six read pulses with an overall reduction to 0.20 compared to a T_2 -weighted series. The rate of T_1 relaxation and choice of recovery times will determine the practical limit to the number of T_1 -weighted stimulated echoes that can be acquired. Since image information is acquired during the recovery time, this will limit the minimum setting of the temporal spacing between read pulses and hence the number of read pulses which can produce useful information. This restriction applies equivalently to the Carr–Purcell T_2 sequence where information is acquired between 180° refocusing pulses.

The slice selection gradient, g_z in Fig. 1, dephases the magnetization during the initial 90° pulse. This dephasing process is refocused by the gradient pulse immediately following the 90° storage pulse and each read pulse. The desired echo obtains its maximum amplitude by this refocusing process and additional undesirable echoes are reduced in strength or eliminated by each successive application of this refocusing gradient. In addition, the four-step phase cycle of Table 1 is performed to allow the discrimination of the sense of precession during phase encoding and to suppress additional signals, not phase encoded, which are generated by the storage and read pulses.

RESULTS

The TART experiment was performed on a phantom of seven bottles filled with water and doped with CuSO_4 to various concentrations. The bottles were approximately 2.5 cm in diameter and the group of seven bottles were stacked so that only the wall thickness separated bottles. The experiments were run on a prototype General Electric CSI imager/spectrometer operating at 85 MHz with a field strength of 2 T. All experiments measured the ^1H resonance of the water.

The pulse sequence of Fig. 1 and phase cycle of Table 1 were performed with four read pulses of the values as given in Table 2. Two-dimensional images were acquired with a field of view of 15 cm in each direction and a slice thickness of 0.2 cm. Each echo was defined with a data block size of 512 points. The image information was collected with 256 phase-encoding steps. With zero filling in both dimensions, this resulted in a final image matrix of 512×512 points. The interval between the peak of the 90° slice selective pulse and the 90° storage was 7.5 ms giving an echo time of 15 ms. The recovery time interval between the 90° storage pulse and first read pulse and between successive read pulses was 50 ms. The entire pulse sequence was repeated every 715 ms. Because of data acquisition limitations of the prototype CSI system, the entire experiment had to be repeated with collection of a single echo each time. The full pulse sequence was used each time so this limitation should not have affected results and only represented a loss of time due to the necessity of repeating the experiment. There is no practical reason why the experiment cannot be performed in a single step on a system modified to acquire data in that form. This modification is presently underway.

Figure 2 represents a comparison of the images obtained with the conventional 90 – 180° spin-echo imaging sequence and that obtained from the primary echo in the TART sequence with the same timing parameters. As expected the primary echo image is reduced in signal-to-noise ratio by a factor of two compared to the conventional spin-echo image. In all images, the horizontal direction represents the phase-encoding gradient direction (x in this case) and the vertical the read-out gradient direction (in

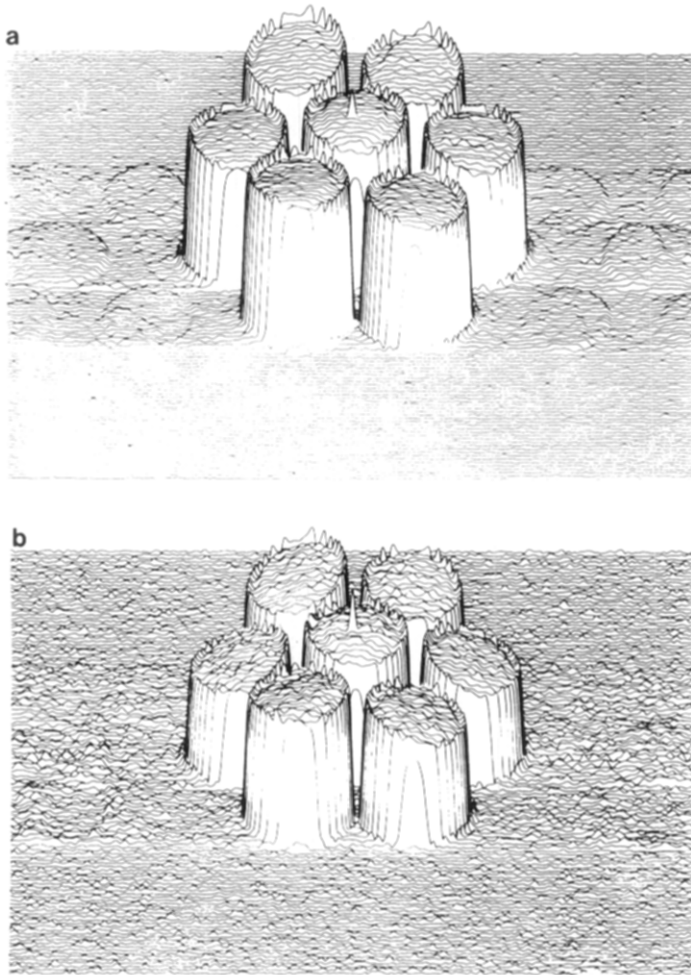


FIG. 2. Comparison of (a) conventional 90–180° spin-echo image and (b) TART 90–90° primary echo image.

this case y). The magnet gradient system is oriented such that x is horizontal and y vertical. The baseline artifacts in the conventional spin-echo image of Fig. 2a are due to gradient instabilities in the phase-encoding gradient. The falloff of intensity in the phase-encoding direction for the TART primary echo image of Fig. 2b is of unknown origin but could be due to rf inhomogeneities. The same effect is not seen in the stimulated echo images following the read pulses in the TART sequence.

The T_1 -weighted series of stimulated echo images for the TART sequence are shown in Fig. 3. The recovery time, RT, progresses in 50 ms steps increasing from 50 ms in Fig. 3a to 200 ms in Fig. 3d. By comparing the image of Fig. 2b with the first image in this T_1 -weighted series, the expected 0.5 loss in signal-to-noise ratio is quite apparent. Qualitatively, the T_1 -weighted series represents the available contrast difference due to variations in longitudinal relaxation rates.

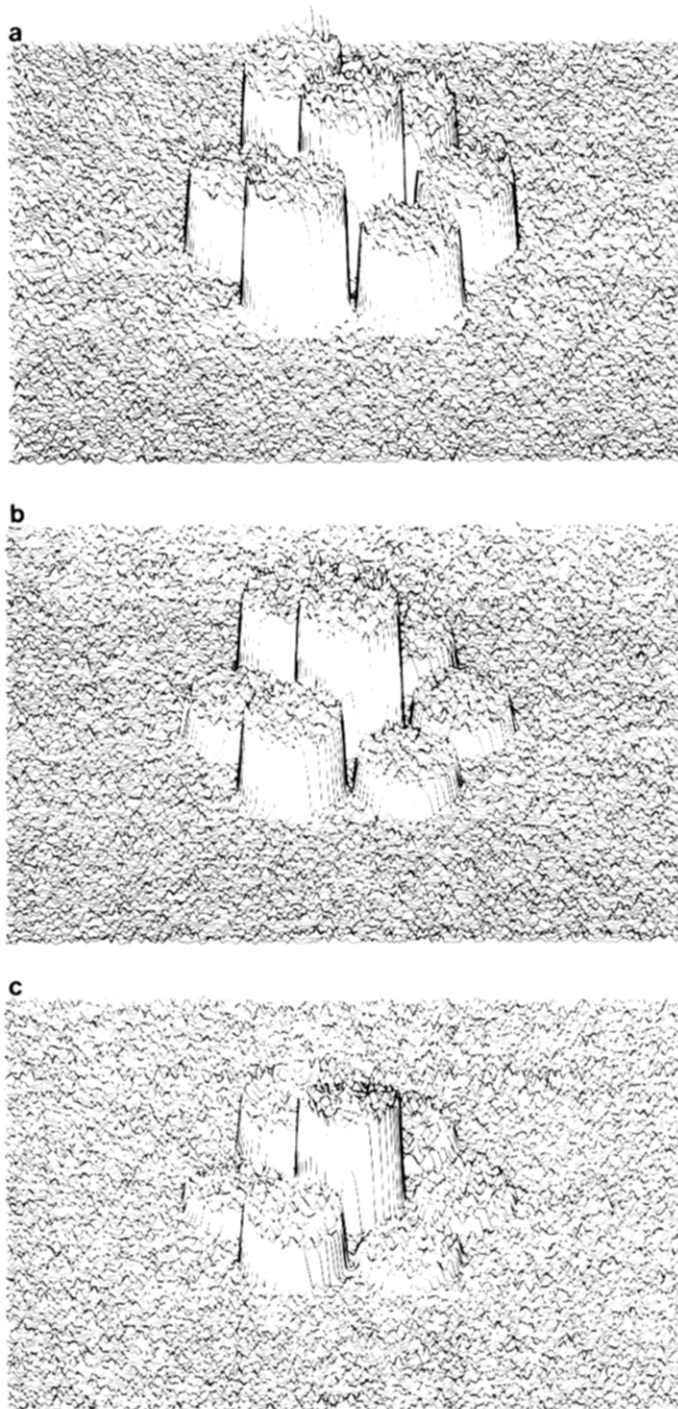


FIG. 3. The T_1 -weighted TART series of images produced by the four read pulse with tip-angle values as given in Table 1. The T_1 recovery time, RT, was equal to (a) 50 ms, (b) 100 ms, (c) 150 ms, and (d) 200 ms.

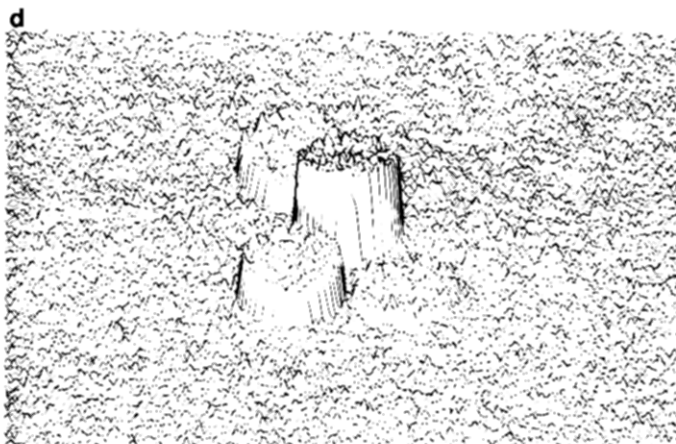


FIG. 3—Continued

To test the quantitative nature of the intensity variations in the TART image series, image intensity values were measured for all seven bottles in each image. These intensity values were determined by averaging pixels over a fixed-size region within the image boundaries of each bottle. The measured intensity values were used to determine the T_1 of each bottle by a two-parameter exponential curve fit to the four data points. The resulting values are shown in the second column of Table 3.

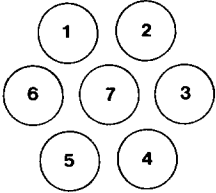
Each bottle was then removed from the phantom and placed in the center of the rf coil and the CSI system operated as a spectrometer without any applied imaging gradients or pulse shaping. The two pulse inversion–recovery T_1 sequence was applied to each bottle separately and eight data points were determined to define the recovery curve. The T_1 value of each bottle was determined by a three-parameter exponential curve fit and the values are reported in the fourth column of Table 3. There is quite good agreement between the two types of measurements indicating the TART sequence produces quantitative results at least in this experimental situation.

The central bottle contained a gel solution to effectively reduce its T_2 . This would have indicated if an unexpected T_2 weighting was contributing to the T_1 weighting in the TART imaging series. The T_2 of this bottle was measured to be 58 ms as compared to the measured T_1 of approximately 230 ms. Since no appropriate reduction in the measured T_1 was observed, the TART sequence appears to have the expected relaxation weighting as described by Eq. [6].

CONCLUSIONS

The TART imaging experiment presented here represents a novel approach to T_1 -weighted imaging which complements the conventional T_2 -weighted spin-echo imaging sequence. The TART sequence has no rf pulses greater than 90° , so slice selection is more easily implemented with this sequence. Multislice, multiecho acquisition should be a straightforward generalization of the sequence in Fig. 1 without the attendant problems of slice selection with 180° pulses. Potentially, the TART sequence can provide a method of quantitative T_1 determination. However, potential problems due to misset tip angles and gradient pulse lengths need to be addressed before the limits

TABLE 3
Calculated T_1 Values of Phantom



Bottle ^a	TART ^b	Standard error ^c	Inversion-recovery ^d	Standard error ^c
1	103	±2.9	115	±0.7
2	66	±1.2	63	±0.09
3	61	±0.9	58	±0.04
4	65	±2.3	63	±0.02
5	117	±7.0	115	±0.7
6	63	±1.6	64	±0.2
7	227	±9.8	246	±1.7

^a All bottles contain tap water doped with various concentrations of CuSO_4 .

^b Values calculated by a two-parameter exponential curve fit to four data points determined by average intensity measurements over a fixed-size region of interest in each of the four images.

^c Standard error in T_1 estimate from exponential curve fit.

^d Values calculated by a three-parameter exponential curve fit to eight data points determined by intensity measurements from a two-pulse inversion-recovery experiment. Each bottle was measured separately by positioning the bottle in the center of the receiver coil and operating the CSI system as a spectrometer.

of accuracy can be determined. In the presence of diffusion, the measured relaxation rate would be a convolution of T_1 relaxation and the rate of diffusion. This is most apparent for relatively long T_1 with large gradients. It should be possible to separate T_1 relaxation and diffusional effects and this problem is presently under study.

Under certain conditions, the number of steps in the phase cycle of Table 1 could be reduced. The first two steps select the echo over the antiecho component of transverse magnetization. This two-step cycle would be unnecessary if either or both the main field inhomogeneity and read-out gradient are large enough to suppress the antiecho component. In this situation, only the echo would be observed during each acquisition and the two-step cycle would be redundant. The third and fourth steps in the phase cycle of Table 1 suppress additional signals from the first two steps, not phase encoded, which are generated by the storage and read pulses. For a well tuned instrument with all pulses slice selective, these additional signals would be negligible and the third and fourth phase-cycling steps could be ignored. The required phase cycle will depend on the specific instrument and under favorable conditions could be reduced to a single-step or at least reduced to a two-step cycle, thus reducing imaging time.

ACKNOWLEDGMENTS

These experiments were performed at General Electric NMR Instruments, Fremont, California, on the applications lab instrument. Special thanks go to Ralph Hurd for his help in performing these experiments and Ellory Schempp for his hospitality during our stay. This research was supported by grants from the National Institutes of Health (P41-RR-02278) and the Veterans Administration Medical Research Service.

REFERENCES

1. P. MANSFIELD AND P. G. MORRIS, *NMR Imaging in Biomedicine*, Academic Press, New York (1982), see Chapter 6.
2. T. L. JAMES AND A. R. MARGULIS (Eds.), "Biomedical Magnetic Resonance," Radiology Research and Education Foundation, San Francisco, 1984.
3. E. L. HAHN, *Phys. Rev.* **76**, 145 (1949).
4. H. Y. CARR AND E. M. PURCELL, *Phys. Rev.* **94**, 630 (1954).
5. S. MEIBOOM AND D. GILL, *Rev. Sci. Instru.* **29**, 688 (1958).
6. E. L. HAHN, *Phys. Rev.* **80**, 580 (1950).
7. W. SATTIN, T. H. MARECI, AND K. N. SCOTT, *J. Magn. Reson.* **64**, 177 (1985); *J. Magn. Reson.* **65**, 298 (1985); J. FRAHM, K. D. MERBOLDT, W. HÄNICKE, AND A. HAASE, *J. Magn. Reson.* **64**, 81 (1985); A. HAASE AND J. FRAHM, *J. Magn. Reson.* **64**, 94 (1985); K. D. MERBOLDT, W. HÄNICKE AND J. FRAHM, *J. Magn. Reson.* **64**, 479 (1985).
8. L. J. FRIEDMAN, Ph.D. Dissertation, Cornell University, Ithaca, N.Y., 1983.
9. A. BAX, T. MEHLKOPF, J. SMIDT, AND R. FREEMAN, *J. Magn. Reson.* **41**, 502 (1980).
10. P. MANSFIELD, *Magn. Reson. Med.* **1**, 370 (1984).